Commun. Comput. Phys.
doi: 10.4208/cicp.060210.270810a

Vol. **10**, No. 2, pp. 405-421
August 2011

# Semiclassical Lattice Boltzmann Simulations of Rarefied Circular Pipe Flows

Jaw-Yen Yang[1,2,*], Li-Hsin Hung[2] and Yao-Tien Kuo[2]

[1] *Center for Quantum Science and Engineering, National Taiwan University, Taipei 106, Taiwan.*
[2] *Institute of Applied Mechanics, National Taiwan University, Taipei 106, Taiwan.*

Received 6 February 2010; Accepted (in revised version) 27 August 2010

Available online 27 April 2011

**Abstract.** Computations of microscopic circular pipe flow in a rarefied quantum gas are presented using a semiclassical axisymmetric lattice Boltzmann method. The method is first derived by directly projecting the Uehling-Uhlenbeck Boltzmann-BGK equations in two-dimensional rectangular coordinates onto the tensor Hermite polynomials using moment expansion method and then the forcing strategy of Halliday et al. [Phys. Rev. E., 64 (2001), 011208] is adopted by adding forcing terms into the resulting microdynamic evolution equation. The determination of the forcing terms is dictated by yielding the emergent macroscopic equations toward a particular target form. The correct macroscopic equations of the incompressible axisymmetric viscous flows are recovered through the Chapman-Enskog expansion. The velocity profiles and the mass flow rates of pipe flows with several Knudsen numbers covering different flow regimes are presented. It is found the Knudsen minimum can be captured in all three statistics studied. The results also indicate distinct characteristics of the effects of quantum statistics.

**AMS subject classifications**: 76P05, 82B40, 82D05, 82C40

**PACS**: 47.11.-j, 51.10.+y, 47.45.Ab, 67.10.Jn

**Key words**: Semiclassical lattice Boltzmann method, axisymmetric flows, rarefied pipe flow, Knudsen minimum.

## 1 Introduction

Over the past two decades, significant advances in the development of the lattice Boltzmann methods (LBMs) [1–4] based on classical Boltzmann equations with the relaxation time approximation of Bhatnagar, Gross and Krook (BGK) [5] have been achieved. The

*Corresponding author. *Email addresses:* `yangjy@spring.iam.ntu.edu.tw` (J.-Y. Yang), `D95543014@ntu.edu.tw` (L.-H. Hung), `t24621@yahoo.com.tw` (Y.-T. Kuo)

 

lattice Boltzmann methods have demonstrated its ability to simulate hydrodynamic systems, magnetohydrodynamic systems, multi-phase and multi-component fluids, multi-component flow through porous media, and complex fluid systems, see [6]. The lattice Boltzmann equations (LBE) can also be directly derived in *a priori* manner from the continuous Boltzmann equations [7, 8]. Most of the classical LBMs are accurate up to the second order, i.e., Navier-Stokes hydrodynamics and have not been extended beyond the level of the Navier-Stokes hydrodynamics. A systematical method [9, 10] was proposed for kinetic theory representation of hydrodynamics beyond the Navier-Stokes equations using Grad's moment expansion method [11].

However, most of the existing lattice Boltzmann methods, despite their great success, are limited to hydrodynamics of classical particles. Recent development in nanoscale transport requires carriers of particles of arbitrary statistics [12]. The generalization of the successful LBMs for classical gas to that for particles of arbitrary statistics is thus desirable. Specifically, a semiclassical Boltzmann equation, which is analogous to the classical Boltzmann equation, for transport phenomenon in quantum gases has been developed by Uehling and Uhlenbeck (UUB) [13]. Also, to avoid the mathematical complexity of the collision term, BGK-type relaxation time models to capture the essential properties of carrier scattering mechanisms can be similarly devised for the Uehling-Uhlenbeck Boltzmann equation for various carriers and have been widely used in carrier transports [14]. Recently, a new semiclassical lattice Boltzmann method for the Uehling-Uhlenbeck Boltzmann-BGK (UUB-BGK) equations based on Grad's moment expansion method by projecting the UUB-BGK equations onto Hermite polynomial basis has been presented [15] for D2Q9 lattice model. Hydrodynamics based on moments up to second and third order expansions are presented. Simulations of flow over a circular cylinder at low Reynolds numbers have been tested and have been found in good agreement with previous available results.

One of the most common and important classes of fluid dynamical problems is the axisymmetric flow in which the flow symmetry with respect to an axis can be identified. Classical axisymmetric lattice Boltzmann method was first proposed by Halliday et al. [16] using a forcing strategy. By introducing source terms, the macroscopic equations for the axisymmetric flows can be recovered through Chapman-Enskog expansion. The method of Halliday et al. has been successfully applied to a number of axisymmetric flow problems [17–25]. Recently, an interesting lattice Boltzmann model for axisymmetric flows based on Boltzmann-BGK equation in cylindrical coordinates has been proposed [26].

The objective of this work is to present the simulation of circular pipe flow in rarefied gases of arbitrary statistics using a semiclassical axisymmetric lattice Boltzmann method. The rarefied circular pipe flows considered here covers the Knudsen $(\lambda \gg D)$, slip $(\lambda \sim D)$ and Poiseuille $(\lambda \ll D)$ regions, where $\lambda$ is the mean free path and $D$ is the pipe diameter. The size-variation effects in transport phenomena occur whenever the mean free path $\lambda$ of the elementary carriers becomes comparable in magnitude to the characteristic dimensions of the system under study. When inter-particle collisions become relatively more frequent organized hydrodynamic flow of the Poiseuille type will compete with the collisionless Knudsen flow. The competition between these two distinct types of flows will be reflected in the appearance of a Knudsen minimum in the mass flow rate as first investigated by Knudsen for a highly rarefied classical gas [27,28]. Thus, another objective of this work is to capture the Knudsen minimum in the rarefied pipe flow of quantum gases of three statistics. The method of Halliday et al. is adopted and forcing terms are added into the two-dimensional semiclassical Boltzmann-BGK equation which are consistent in dimension with the lattice Boltzmann equation. The forcing terms are determined by demanding the emergent macroscopic equations toward a particular target form. The set of correct macroscopic equations for incompressible axisymmetric flows can be recovered through the Chapman-Enskog multiscale analysis of the semiclassical LBM.

This paper is organized as follows. A brief description of element of semiclassical kinetic theory is given in Section 2. The basic two-dimensional semiclassical lattice Uehling-Uhlenbeck Boltzmann-BGK method is described in Section 3. The derivation of the axisymmetric semiclassical LBM is given in Section 4. Simulations of circular pipe flows over a wide range of Knudsen numbers are presented in Section 5. Concluding remarks are given in Section 6. The detailed Chapman-Enskog multiscale analysis and derivation of the method are given in an Appendix.

## 2 Semiclassical Boltzmann-BGK equation

We consider the Uehling-Uhlenbeck Boltzmann-BGK equation

$$\frac{\partial f}{\partial t}+\frac{\vec{p}}{m}\cdot\nabla_{\vec{x}}f=-\frac{\left(f-f^{(eq)}\right)}{\tau^*},\tag{2.1}$$

where $m$ is the particle mass, $f(\vec{p},\vec{x},t)$ is the distribution function which represents the average density of particles with momentum $\vec{p}$ at the space-time point $\vec{x},t$. In Eq. (2.1), $\tau^*$ is the relaxation time which is in general dependent on the macroscopic variables and $f^{(eq)}$ is the local equilibrium distribution given by

$$f^{(eq)}=\left\{\exp\left[\frac{(\vec{p}-m\vec{u})^2}{2mk_BT}-\frac{\bar{\mu}}{k_BT}\right]-\theta\right\}^{-1},\tag{2.2}$$

where $\vec{u}$ is the mean macroscopic velocity, $T$ is the temperature, $\bar{\mu}$ is the chemical potential, $k_B$ is the Boltzmann constant and $\theta=-1$ denotes the Fermi-Dirac (FD) statistics, $\theta=+1$ the Bose-Einstein (BE) statistics and $\theta=0$, the Maxwell-Boltzmann (MB) statistics. Once the distribution function is known, the macroscopic quantities, the number density $n$, number density flux $n\vec{u}$, energy density $\epsilon$, pressure tensor $P_{\alpha\beta}$, and heat flux vector $Q_\alpha$ are defined, respectively, by

$$\Phi(\vec{x},t)=\int\frac{d\vec{p}}{h^3}\phi f,\tag{2.3}$$

where $\Phi=(n,n\vec{u},\epsilon,P_{\alpha\beta},Q_\alpha)^T$ and $\phi=(1,\vec{\xi},mc^2/2,c_\alpha c_\beta,mc^2c_\alpha/2)^T$. Here, $\vec{\xi}=\vec{p}/m$ is the particle velocity and $\vec{c}=\vec{\xi}-\vec{u}$ is the thermal velocity. The gas pressure is defined by $P(\vec{x},t)=P_{\alpha\alpha}/3=2\epsilon/3$. Multiplying Eq. (2.1) by $1,\vec{p}$, or $\vec{p}^2/2m$, and integrating the resulting equations over all $\vec{p}$, then one can obtain the semiclassical hydrodynamical equations,

$$\frac{\partial n}{\partial t}+\nabla_{\vec{x}}\cdot(n\vec{u})=0, \tag{2.4}$$

$$mn\Big(\frac{\partial}{\partial t}+\vec{u}\cdot\nabla_{\vec{x}}\Big)u_\alpha=-\frac{\partial P}{\partial x_\alpha}+\frac{\partial}{\partial x_\beta}\Big\{2\eta\Big[D_{\alpha\beta}-\frac{1}{3}(TrD)\delta_{\alpha\beta}\Big]\Big\}, \tag{2.5}$$

$$\frac{\partial \epsilon}{\partial t}+\nabla_{\vec{x}}\cdot(\epsilon\vec{u})+(\nabla_{\vec{x}}\cdot\vec{u})P=\nabla_{\vec{x}}\cdot(\kappa\nabla T)+2\eta\Big[D_{\alpha\beta}-\frac{1}{3}(TrD)\delta_{\alpha\beta}\Big]^2, \tag{2.6}$$

where $D_{\alpha\beta}=(\partial u_\alpha/\partial x_\beta+\partial u_\beta/\partial x_\alpha)/2$ is the rate of strain tensor, $Tr$ denotes the trace of tensor $D_{\alpha\beta}$, and $\eta$ and $\kappa$ are the viscosity and thermal conductivity, respectively.

The viscosity $\eta$ and thermal conductivity $\kappa$ for the semiclassical Boltzmann BGK model have been derived in [29] based on the Chapman-Enskog solution [30] in terms of the relaxation time as

$$\eta=\tau^* nk_BT\frac{g_{\frac{5}{2}}(\bar{z})}{g_{\frac{3}{2}}(\bar{z})}, \tag{2.7}$$

$$\kappa=\tau^*\frac{5k_B}{2m}nk_BT\Big[\frac{7}{2}\frac{g_{\frac{7}{2}}(\bar{z})}{g_{\frac{3}{2}}(\bar{z})}-\frac{5}{2}\frac{g_{\frac{5}{2}}(\bar{z})}{g_{\frac{3}{2}}(\bar{z})}\Big]. \tag{2.8}$$

Here $\bar{z}(\vec{x},t)=e^{\bar{\mu}(\vec{x},t)/k_BT}$ is the fugacity. The function $g_\nu$ represents for either the Bose-Einstein or Fermi-Dirac function of order $\nu$ which is defined as

$$g_\nu(\bar{z})\equiv\frac{1}{\Gamma(\nu)}\int_0^\infty\frac{x^{\nu-1}}{\bar{z}^{-1}e^x+\theta}dx=\sum_{l=1}^{\infty}(-\theta)^{l-1}\frac{\bar{z}^l}{l^\nu}, \tag{2.9}$$

where $\Gamma(\nu)$ is the Gamma function. The relaxation times for various scattering mechanisms of different carrier transport in semiconductor devices including electrons, holes, phonons and others have been proposed [14].

In this work, we consider the semiclassical incompressible viscous flows with rotational symmetry around the $z$ axis. The cylindrical polar coordinates $\vec{x}=(r,\phi,z)$ system is adopted where $r$ denoting the radial distance from axis, $\phi$ the azimuthal angle about axis and $z$ the distance along the axisymmetric axis, respectively. The mean velocity is $\vec{u}=(u_r,0,u_z)$. The governing equations for the incompressible (constant $n$ or $\rho$) axisymmetric viscous flows in a cylindrical polar coordinates system can be expressed as

$$\frac{\partial u_j}{\partial x_j}=-\frac{u_r}{r}, \tag{2.10}$$

$$\frac{\partial u_i}{\partial t}+u_j\frac{\partial u_i}{\partial x_j}=-\frac{1}{\rho}\frac{\partial P}{\partial x_i}+\eta\frac{\partial^2 u_i}{\partial x_j^2}+\frac{\eta}{r}\frac{\partial u_i}{\partial r}-\frac{\eta u_i}{r^2}\delta_{ir}. \tag{2.11}$$

Inserting the continuity equation into the momentum equation, we have

$$\frac{\partial u_i}{\partial t}+\frac{\partial(u_iu_j)}{\partial x_j}=-\frac{1}{\rho}\frac{\partial P}{\partial x_i}+\eta\frac{\partial^2 u_i}{\partial x_j^2}-\frac{u_iu_r}{r}+\frac{\eta}{r}\frac{\partial u_i}{\partial r}-\frac{\eta u_i}{r^2}\delta_{ir}. \tag{2.12}$$

The aim of this work in the following is first to derive a semiclassical lattice Boltzmann equation which shall render the macroscopic continuity and momentum equations, Eqs. (2.10) and (2.12), self-consistently and second to apply the method to compute rarefied circular pipe flows in gases of arbitrary statistics. We note that the axisymmetric Navier-Stokes equations, Eq. (2.10) and Eq. (2.12) have the 2-D Navier-Stokes equations embedded. Similarly, the axisymmetric lattice Boltzmann method will also have the 2-D method embedded. For this reason, we shall first briefly describe the 2-D semiclassical lattice Boltzmann method in the next Section, for further details see [15].

## 3 A semiclassical lattice Boltzmann-BGK method

In [15], a semiclassical lattice Boltzmann method (SLBM) based on D2Q9 lattices in rectangular coordinates for gases of particles of arbitrary statistics has been developed. Since the axisymmetric method has the 2-D method embedded in general. Here, for completeness, we include some brief description of the essential elements of the method and use it as the basis to extend to the axisymmetric case. The Grad's moment approach was adopted to find solutions to Eq. (2.1) by expanding $f(\vec{x},\vec{\zeta},t)$ in terms of Hermite polynomials and the $N$-th finite order truncated distribution function $f^N$ was considered. The expansion of the distribution function $f$ to the $N$-th order can be expressed by

$$f^N(\vec{x},\vec{\zeta},t)=\omega(\vec{\zeta})\sum_{n=0}^{N}\frac{1}{n!}\mathbf{a}^{(n)}(x,t)\mathcal{H}^{(n)}(\vec{\zeta}), \tag{3.1}$$

where $\vec{\zeta}\equiv\vec{p}/h^3$, $\omega(\vec{\zeta})=(2\pi)^{-3/2}e^{-\vec{\zeta}^2/2}$ is the weighting function, $\mathbf{a}^{(n)}$ and $\mathcal{H}^{(n)}(\vec{\zeta})$ are rank-n tensors and the product on the right-hand side denotes full contraction. The expansion coefficients $\mathbf{a}^{(n)}$ are given by

$$\mathbf{a}^{(n)}(\vec{x},t)=\int f^N(\vec{x},\vec{\zeta},t)\mathcal{H}^{(n)}(\vec{\zeta})d\vec{\zeta}, \tag{3.2}$$

where $d\vec{\zeta}=d\vec{p}/h^3$. Similarly, the equilibrium distribution function $f^{(eq)}$ can be expanded to the same order as $f$ and normally can be analytically found in terms of Fermi or Bose function. The standard square D2Q9 lattice model is used:

$$\vec{\zeta}_0=(0,0), \tag{3.3a}$$

$$\vec{\zeta}_a=\Big(\cos\Big(\frac{a-1}{4}\Big)\pi,\sin\Big(\frac{a-1}{4}\Big)\Big)c,\quad a=1,\cdots,8, \tag{3.3b}$$

where $c=\delta_z/\delta_t$ is the particle streaming speed and $\delta_z$ is the lattice size and $\delta_t$ is the time step. When $c$ is taken as 1, the lattice velocity $\vec{\zeta}_a=(\zeta_{az},\zeta_{ar})$ has unit magnitude for directions of $a$=1,3,5 and 7, and magnitude $\sqrt{2}$ for directions of $a$=2,4,6, and 8. For $N$=3, we get the explicit Hermite expansion of the Bose-Einstein (or Fermi-Dirac) distribution at the discrete velocity $\vec{\zeta}_a$ as:

$$f_a^{(eq)}(\vec{x},t)=w_a n\Big\{1+\vec{\zeta}_a\cdot\vec{u}(\vec{x},t)+\frac{1}{2}\Big[(\vec{u}(\vec{x},t)\cdot\vec{\zeta}_a)^2-u^2(\vec{x},t)+\Big(\hat{T}(\vec{x},t)\frac{g_{\frac{5}{2}}(\bar{z})}{g_{\frac{3}{2}}(\bar{z})}-1\Big)(\zeta_a^2-D)\Big]$$
$$+\frac{\vec{\zeta}_a\cdot\vec{u}}{6}\Big[(\vec{u}\cdot\vec{\zeta}_a)^2-3u^2+3\Big(\hat{T}\frac{g_{\frac{5}{2}}(\bar{z})}{g_{\frac{3}{2}}(\bar{z})}-1\Big)(\zeta_a^2-D-2)\Big]\Big\}, \tag{3.4}$$

where $D=\delta_{ii}$ and $\hat{T}$ is the non-dimensional temperature. A lattice UUB-BGK method for solving Eq. (2.1) as constructed in [15] is expressed as

$$f_a(\vec{x}+\vec{\zeta}_a\delta_t,t+\delta_t)-f_a(\vec{x},t)=-\frac{1}{\tau}\big[f_a-f_a^{(eq)}\big], \tag{3.5}$$

where $\tau=\tau^*/\delta_t$ is the dimensionless LBE relaxation time.

Once we have solved the new time values of $f_a(\vec{x},t)$, the macroscopic variables such as $n(\vec{x},t)$,$\vec{u}(\vec{x},t)$ and $\hat{T}(\vec{x},t)$, can be calculated by:

$$n(\vec{x},t)=\sum_{a=1}^{l} f_a(\vec{x},t), \tag{3.6}$$

$$n\vec{u}=\sum_{a=1}^{l} f_a\vec{\zeta}_a, \tag{3.7}$$

$$n\Big(D\hat{T}\frac{g_{\frac{5}{2}}(\bar{z})}{g_{\frac{3}{2}}(\bar{z})}+u^2\Big)=\sum_{a=1}^{l} f_a\zeta_a^2=E. \tag{3.8}$$

The above three equations provide a way to determine the fugacity $\bar{z}$ through an iteration method,

$$E-3\Big(\frac{n}{g_{\frac{3}{2}}}\Big)^{\frac{5}{3}}g_{\frac{5}{2}}-nu^2=0. \tag{3.9}$$

After obtaining $\bar{z}$, we can get the temperature $\hat{T}$. These quantities are required in the local equilibrium distribution function $f_a^{(eq)}$ of Eq. (3.4).

Now we are ready to generalize to axisymmetric case based on the above two-dimensional semiclassical LBM in rectangular coordinates.

## 4 Semiclassical axisymmetric lattice Boltzmann method

As we noted before, the axisymmetric lattice Boltzmann method will have the 2-D lattice Boltzmann method embedded. To derive the semiclassical axisymmetric lattice Boltzmann method, we construct the method based on the above 2-D semiclassical lattice

Boltzmann method and adopt the approach of Halliday et al. by incorporating a position and time dependent source or sink term into the microdynamic evolution equation as follows:

$$f_a(\vec{x}+\vec{\zeta}_a\delta_t,t+\delta_t)-f_a(\vec{x},t)=-\frac{1}{\tau}[f_a-f_a^{(eq)}]+h_a(\vec{x},t), \tag{4.1}$$

where the 2-D equation is embedded and $h_a(\vec{x},t)$ is an added source or sink term that will be defined later. Following the analysis of [16], we assume

$$h_a=\varepsilon h_a^{(1)}+\varepsilon^2 h_a^{(2)}+\cdots, \tag{4.2}$$

and take $h_a^{(1)}$ to be zeroth order in gradient quantities and $h_a^{(2)}$ to contain any first order gradients in macroscopic dynamic quantities $n,\vec{u}$; that is $h_a^{(n)}$ contains $(n-1)$-th order gradients in $n$ and $\vec{u}$. The issue now is to determine the $h_a^{(n)}$ that will render Eqs. (2.10) and (2.12) in a self-consistent manner.

To extract the dynamics represented by this modifying scheme, one has to rely on the Chapman-Enskog multiscale analysis. Here we first summarize the complete basic equations and the detailed derivations are provided in the Appendix.

From Appendix, we have $h_a^{(1)}$ as follow:

$$h_a^{(1)}=-\frac{w_a n u_r}{r}\delta_t. \tag{4.3}$$

With this choice of $h_a^{(1)}$, then we have

$$\sum_a h_a^{(1)}=-\frac{n u_r}{r}. \tag{4.4}$$

We also have $h_a^{(2)}$ as following:

$$\begin{aligned} h_a^{(2)}=&\frac{\partial u_r}{\partial r}\left[\delta_t u_r+\frac{\zeta_{ar}}{r}+\frac{\zeta_{ar}(2\mu-\delta_t\tau)}{r}\right]nw_a\delta_t+\frac{\partial u_z}{\partial r}\left[\frac{\mu\zeta_{az}}{r}\right]nw_a\delta_t\\ &+\frac{\partial u_r}{\partial z}\left[\frac{1}{2}u_z\delta_t+\frac{\zeta_{az}(2\mu-\delta_t\tau)}{r}\right]nw_a\delta_t+\frac{\partial u_z}{\partial z}\frac{1}{2}\delta_t u_r\delta_t n w_a\\ &-nw_a\delta_t\left[\frac{u_r^2\zeta_{ar}}{r}+\frac{u_r u_z\zeta_{az}}{r}+\frac{\mu u_r\zeta_{ar}}{r^2}+\frac{u_r\zeta_{ar}(2\mu-\delta_t\tau)}{r^2}\right]. \end{aligned} \tag{4.5}$$

The derivative terms in Eq. (4.5) can be evaluated using the following:

$$\frac{\partial u_r}{\partial r}=\frac{1}{2}\left[-\frac{1}{\tau n\Theta}\sum_a\zeta_{ar}\zeta_{ar}f_a^{(1)}+\frac{u_r}{r}\left(1-\frac{1}{\Theta}\right)\right], \tag{4.6}$$

$$\frac{\partial u_z}{\partial z}=\frac{1}{2}\left[-\frac{1}{\tau n\Theta}\sum_a\zeta_{az}\zeta_{az}f_a^{(1)}+\frac{u_r}{r}\left(1-\frac{1}{\Theta}\right)\right], \tag{4.7}$$

$$\frac{\partial u_z}{\partial r}=\frac{1}{2}\left[-\frac{1}{\tau n\Theta}\sum_a\zeta_{az}\zeta_{ar}f_a^{(1)}+\frac{u_r}{r}\left(1-\frac{1}{\Theta}\right)\right], \tag{4.8}$$

$$\left(\frac{\partial u_r}{\partial z}\right)_{r,z}=\frac{(u_r)_{r,z+1}-(u_r)_{r,z-1}}{2\delta_z}. \tag{4.9}$$

It is noted that only one derivative term has to be computed using finite (central) difference method and the rest of derivative terms can be analytically expressed and directly computed. To complete the derivation, we set

$$h_a = \delta_t h_a^{(1)} + \delta_t^2 h_a^{(2)}$$

in Eq. (4.2) to achieve the final semiclassical lattice Boltzmann method (SLBM) for axisymmetric flows.

In summary, Eqs. (4.1), (4.3) and (4.5) form a closed set of differential equations governing the set of variables $f_a(\vec{x},t)$ in the physical configuration space and the correct hydrodynamic equations can be obtained via the Chapman-Enskog analysis. All the macroscopic variables and their fluxes can be calculated directly from their corresponding moment summations.

A major issue about using SLBM to simulate the micro flows is the treatment of wall boundary condition. Bounce-back scheme is often used to realize non-slip boundary condition in Poiseuille region while the specular reflection scheme is applied to free-slip boundary condition where no momentum is to be exchanged with the wall along the tangential component. For realistic flow in microtubes, a combination of the two schemes is usually considered by defining the parameter $0 \leq \sigma \leq 1$. For example, we have $f_2(i,1) = f_4(i,1), f_5(i,1) = \sigma f_7(i,1) + (1-\sigma) f_8(i,1)$ and $f_6(i,1) = \sigma f_8(i,1) + (1-\sigma) f_7(i,1)$. For $\sigma = 1$, there is no slip at wall and we have the bounce-back scheme; for $\sigma = 0$, we have the specular reflection scheme. The choice of $\sigma$ is usually done by matching with experimental data.

To apply Eq. (4.1), one has to determine either $\tau$ or $\tau^*$. For continuum flows, one can perform Chapman-Enskog multiscale analysis to Eq. (4.1), and $\tau$ is determined in such a way that the Navier-Stokes equations are recovered. As a result, we have the relaxation time $\tau$ related to the fluid viscosity $\nu$ as

$$\nu = \left(\tau - \frac{1}{2}\right) \hat{T} \frac{g_{\frac{5}{2}}}{g_{\frac{3}{2}}}, \tag{4.10}$$

where $\nu$ is the non-dimensional kinematic viscosity. The term $-1/2$ in the above equation is a correction to make the LBE technique a second-order method for solving incompressible flows.

## 5 Results and discussion

We consider a uniform pressure-driven circular pipe flow in a rarefied quantum gas. The pipe length is $L$ and diameter $D$ and $L/D = 25$. With the given fugacity at the inlet $\bar{z}_{in} = 0.2$ for all three statistics, we have $\bar{z}_{out} = 0.09835$ for the Fermi gas, $\bar{z}_{out} = 0.101913$ for the Bose gas, and $\bar{z}_{out} = 0.1$ for the classical limit. The inlet temperature is $T_{in} = 0.5$ and outlet

$T_{out}=0.5$, then the pressure ratio will be

$$\Big(\frac{P_{in}}{P_{out}}\Big)=\Big(nT\frac{g_{\frac{5}{2}}(\bar{z})}{g_{\frac{3}{2}}(\bar{z})}\Big)_{in}\Big/\Big(nT\frac{g_{\frac{5}{2}}(\bar{z})}{g_{\frac{3}{2}}(\bar{z})}\Big)_{out}=\frac{g_{\frac{5}{2}}(\bar{z}_{in})}{g_{\frac{5}{2}}(\bar{z}_{out})}=2$$

for the three cases. The pressure gradient $\Delta P=0.0001832$. Since the D2Q9 square lattice is applied, $L$ can be written as $L=(N_z-1)\delta_z$, and $D=(N_r-1)\delta_r$, where $N_z$ and $N_r$ are the number of lattice nodes in the $z$- and $r$-direction, respectively. To begin with the computation, the desired $Kn=\lambda/D$ is first set. We also set the lattice spacing $\delta_z=\delta_r=1$. The relaxation time $\tau$ can be expressed as

$$\tau=Kn(N_r-1). \tag{5.1}$$

Having $Kn$ defined, appropriate $N_r$ and $\tau$ could be chosen, which could then be used in the determination of mesh size and the collision propagation updating procedure, respectively. The computation domain is $(0\le z\le 524,\ 0\le r\le 20)$ and $525\times 21$ uniform lattices were used. We assume $\sigma=0.75$ at the pipe wall for all the results shown below. Cases for other values of $\sigma$ can be easily calculated. Several Knudsen numbers covering Poiseuille continuum, slip, transition and Knudsen flow regimes are calculated. The so-called size-variation effects in transport phenomena occur in highly rarefied classical gas as first investigated by Knudsen will be studied using the present semiclassical lattice Boltzmann method. Markedly distinct behaviors were observed due to different inter-particles or particle-wall scattering. In particular, the appearance of a Knudsen minimum in the mass flow rate [27,28] was observed. We note that the Fermi-gas analog of the classical result was also reported before [31]. Here, we report some results for the general type of carriers.

The steady velocity profiles for the three statistics, BE, MB, and FD gases for the case of $\bar{z}=0.2$ are shown in Fig. 1, respectively, for three different Knudsen numbers to represent the Knudsen, slip and Poiseuille regions. For the small Knudsen number, $Kn=0.06$, the characteristic parabolic velocity profile is evident. For $Kn=0.2$, the velocity is smaller than that of $Kn=0.6$ and velocity slip at the walls can be identified. For $Kn=1.0$, the velocity peak at the centerline is slightly larger than that of $Kn=0.2$. The velocity slip at wall can be clearly observed. At even larger Knudsen number $Kn=2.0$, the velocity at centerline is getting larger and the velocity slip at wall is large. It can be found that the profile for MB gas lies always in between that of the BE and FD gas and for small Knudsen number, the three profiles get closer to each other.

The mass flow rates for all three statistics, BE, MB, and FD gases for the case of $\bar{z}=0.2$ for Knudsen number covering Knudsen, slip and Poiseuille regimes are shown in Fig. 2. Seven values of Knudsen number from 0.06 to 2.0 were calculated. The Knudsen minimum can be clearly identified for all three statistics and the profile for MB gas lies always in between that of the BE and FD gas. The Knudsen minimum is found to occur at the $Kn=0.4$ case. Basically, the Knudsen minimum of a pipe of channel flow can be viewed

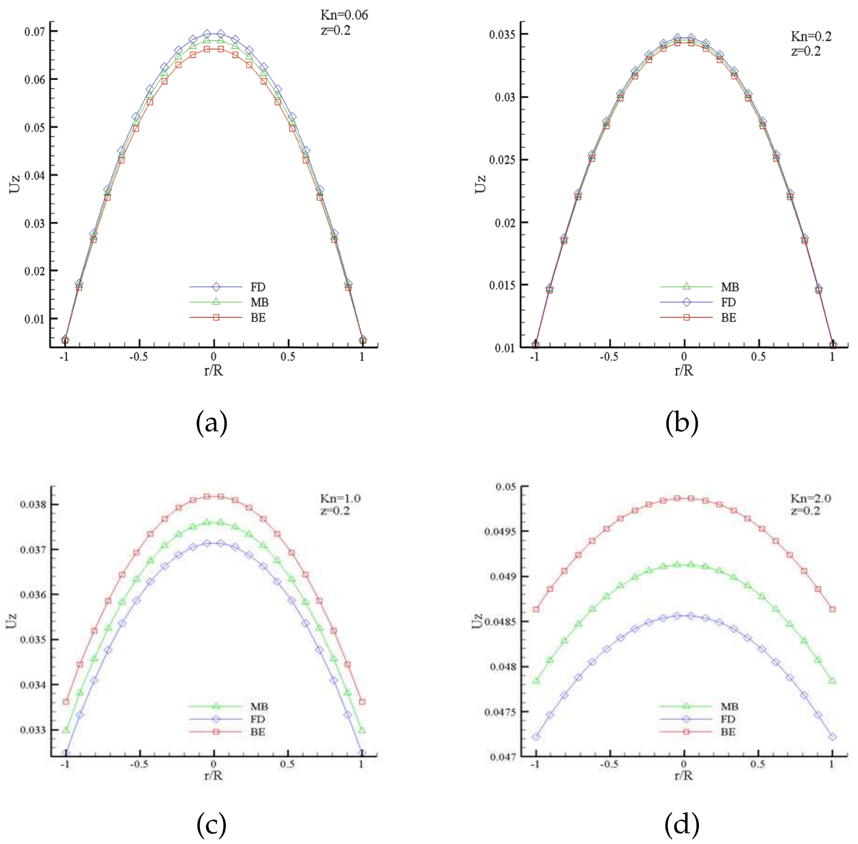


Figure 1: Velocity profiles in a circular pipe flow of gases of arbitrary statistics (gas with $\bar{z}=0.2$). (a) Kn=0.06, (b) Kn=0.2, (c) Kn=1.0, (d) Kn=2.0.

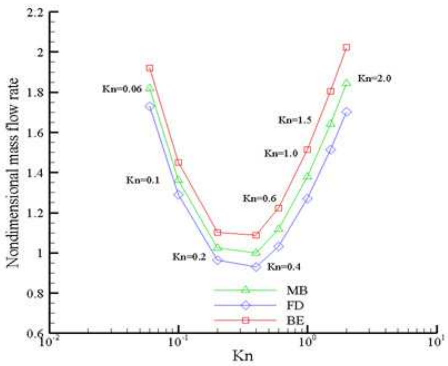


Figure 2: Normalized mass flux in a circular pipe flow as a function of $Kn$ number (gas with $\bar{z}=0.2$).

and explained as a phenomena that appears when the flow passing through the competition between the classical Poiseuille continuum flow and the Knudsen flow and the value of Knudsen number at this minimum should lie in the slip and transition regime.

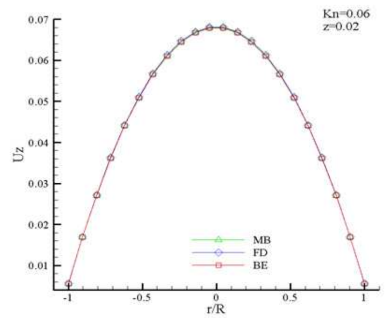


(a)

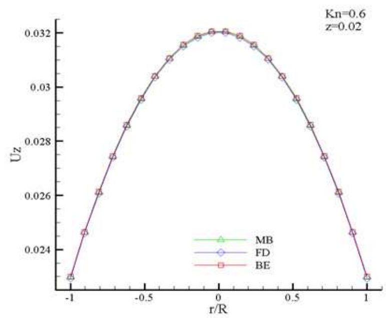


(b)

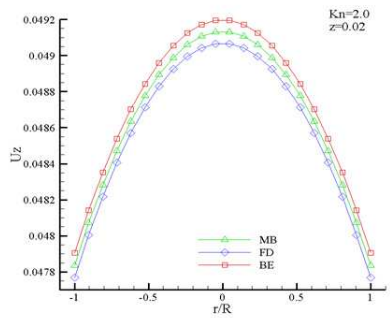


(c)

Figure 3: Velocity profiles in a circular pipe flow of gases of arbitrary statistics (gas with $\bar{z}=0.02$). (a) Kn=0.06, (b) Kn=0.6, (c) Kn=2.0.

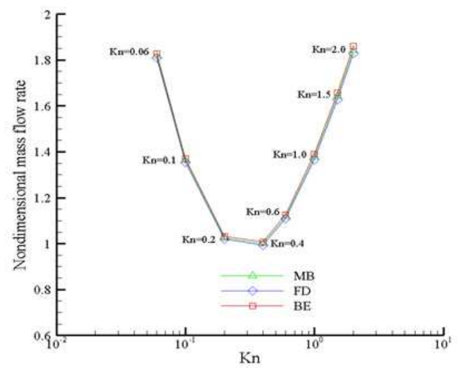


Figure 4: Normalized mass flux in a circular pipe flow as a function of $Kn$ number (gas with $\bar{z}=0.02$).

It is also found that the Knudsen number value at Knudsen minimum is very sensitive to the specularity condition (specified by $\sigma$) of the wall surface. Our value obtained here is in agreement with that reported in the literatures (see [31–33]). For example, in [31], first observation of the Knudsen minimum in normal liquid $^3He$ was reported and the position of Knudsen minimum was found to lie at Knudsen number of $\simeq 0.5$ as compared to the value of 0.75. Also, Knudsen minima for phonons at Knudsen numbers of $0.87\pm0.13$ and 0.65, respectively, have been reported, see [32,33]. Other Knudsen values of Knudsen minimum in liquid $^3He$ in the Knudsen and Poiseuille regions for various specular scattering coefficients were reported [34].

To further test the method, we also compute the case for smaller value of fugacity, $\bar{z}_{in}=0.02$, which corresponds to near classical limit. The grid system and the flow parameters are all the same as the previous $\bar{z}_{in}=0.2$ case. Here, $\bar{z}_{in}=0.02$, $\bar{z}_{out,MB}=0.01$,$\bar{z}_{out,FD}=0.00998$, and $\bar{z}_{out,BE}=0.010078$. The value of $\sigma=0.75$ was used at pipe wall. The velocity profiles at several Knudsen numbers for the three statistics are plotted in Fig. 3. For $Kn=0.06$ and $Kn=0.6$, the velocity profiles of the three statistics almost coincide with each other, though the maximum velocity at the centerline for $Kn=0.06$ is twice as large. There is some velocity slip for the $Kn=0.6$ case. For the $Kn=2.0$ case, the three statistics display noticeable difference and the velocity slip is very obvious. The mass flow rates for several Knudsen numbers are shown in Fig. 4. We can see that for smaller value of $\bar{z}$, we are getting closer to classical limit and the three statistics indicate similar trend, particularly the mass flow rate which is almost identical. Again, the Knudsen minimum can be clearly captured for all three statistics and the Knudsen minimum is found to occur at the $Kn=0.4$ case.

Theoretically, as comparing with particles of classical statistics, the effects of quantum statistics at finite temperatures (non-degenerate case) are approximately equivalent to introducing an interaction between particles [35]. This interaction is attractive for bosons and repulsive for fermions and operates over distances of order of the thermal wavelength $\Lambda$. Our present simulation examples seem to be able to illustrate and explore the manifestation of the effect of quantum statistics.

## 6 Concluding remarks

The flows of gases of particles of arbitrary statistics in a circular pipe flow are investigated using an axisymmetric semiclassical lattice Boltzmann-BGK method. The method is derived based on a previous D2Q9 semiclassical lattice Boltzmann method and the forcing strategy of Halliday et al. [16] is adopted by adding forcing terms to modify the emergent macroscopic equations toward axisymmetric governing equations. The equilibrium distribution of lattice Boltzmann equations is derived through expanding the Bose-Einstein (or Fermi-Dirac) distribution function onto Hermite polynomial basis up to the same order consistent with the velocity distribution function. The procedure is done in *a priori* manner and is free of usual *ad hoc* parameter-matching. Moreover, our development recovers previous classical results when the classical limit is taken. Computations of micro circular pipe flows in both Bose-Einstein and Fermi-Dirac gases have been simulated. The velocity profiles and mass flow rates for wide range of Knudsen numbers covering Knudsen, transition, slip, and Poiseuille regimes are detailed. The Knudsen minimum phenomena in a circular pipe flow can be captured for all the three particle statistics and the effect of quantum statistics on the hydrodynamics is clearly delineated. Our finding is consistent with some previous results on Knudsen minimum for quantum gases [31].

Also, our results are obtained based on a rather systematic and parallel treatment of all statistics, hence it can be consistently examined within the theory itself among the three statistics.

## Acknowledgments

This work was supported by CQSE Subproject #5 97R0066-69 and NSC 97-2221-E002-063-MY3. They also acknowledge the support of NCHC in providing resource under the national project "Knowledge Innovation National Grid" in Taiwan are acknowledged.

## Appendix to Section 4 derivation of forcing terms

According to the Chapman-Enskog expansion, $f_a$ can be expressed in a series of $\varepsilon$,

$$f_a(\vec{x}+\vec{\zeta}_a\delta_t, t+\delta_t)=\sum_0^\infty \frac{\varepsilon^n}{n!}(\partial_t+\vec{\zeta}_a\cdot\nabla)^n f_a, \tag{A.1}$$

$$f_a \backsimeq f_a^{(0)}+\varepsilon f_a^{(1)}+\varepsilon^2 f_a^{(2)}+\cdots, \tag{A.2}$$

$$\partial_t=\varepsilon\partial_{t_1}+\varepsilon^2\partial_{t_2}, \tag{A.3}$$

$$\partial_\beta=\varepsilon\partial_{\beta_1}. \tag{A.4}$$

The above expressions of the derivatives, Eqs. (A.1)-(A.4) are substituted into Eq. (4.1), and terms involving different orders of $\varepsilon$ are separated as:

$$f_a^{(0)}=f_a^{(eq)}, \tag{A.5}$$

$$(\partial_{t_1}+\zeta_{a\beta}\cdot\partial_{\beta_1})f_a^{(0)}=-\frac{1}{\tau\delta_t}f_a^{(1)}+\frac{h_a^{(1)}}{\delta_t}, \tag{A.6}$$

$$\partial_{t_2}f_a^{(0)}+\Big(1-\frac{1}{2\tau}\Big)(\partial_{t_1}+\zeta_{a\beta}\partial_{\beta_1})f_a^{(1)}+\frac{1}{2}(\partial_{t_1}+\zeta_{a\beta}\partial_{\beta_1})h_a^{(1)}=-\frac{1}{\tau\delta_t}f_a^{(2)}+\frac{h_a^{(2)}}{\delta_t}. \tag{A.7}$$

We have the usual conditions

$$\sum_a f_a=\sum_a f_a^{(eq)}=n, \tag{A.8}$$

$$\sum_a f_a\zeta_a=\sum_a f_a^{(eq)}\zeta_a=n\vec{u}, \tag{A.9}$$

$$\sum_a f_a\zeta_{ai}\zeta_{aj}=\sum_a f_a^{(eq)}\zeta_{ai}\zeta_{aj}=n(u_iu_j+\Theta\delta_{ij}), \tag{A.10}$$

$$\sum_a f_a\zeta_{ai}\zeta_{aj}\zeta_{aj}=n\Theta(u_i\delta_{jk}+u_j\delta_{ki}+u_k\delta_{ij}), \tag{A.11}$$

where $\Theta=\hat{T}g_{5/2}/g_{3/2}$. For $l\geq 1$, we have

$$\sum_a f_a^{(l)}=0, \qquad \sum_a f_a^{(l)}\zeta_a=0. \tag{A.12}$$

### A.1 Lattice continuity equation and $h_a^{(1)}$

We take the moment of Eq. (A.6) and Eq. (A.7), the different order mass conservation equations are recovered below:

$$\partial_{t_1}\sum_a f_a^{(0)}+\partial_{\beta_1}\sum_a f_a^{(0)}\zeta_{a\beta}=-\frac{1}{\tau}\sum_a f_a^{(1)}+\sum_a h_a^{(1)}, \tag{A.13}$$

$$\partial_{t_2}\sum_a f_a^{(0)}+\sum_a\Big[\frac{1}{2}(\partial_{t_1}+\zeta_{a\beta}\partial_{\beta_1})h_a^{(1)}-\frac{1}{\delta_t}h_a^{(2)}\Big]=0. \tag{A.14}$$

If we set the following constraint:

$$\sum_a\Big[\frac{1}{2}(\partial_{t_1}+\zeta_{a\beta}\partial_{\beta_1})h_a^{(1)}-\frac{1}{\delta_t}h_a^{(2)}\Big]=0. \tag{A.15}$$

Then, we have

$$\partial_{t_2}\sum_a f_a^{(0)}=0. \tag{A.16}$$

We have the conservation of mass, i.e., the continuity equation

$$\partial_t n+\delta_t\partial_\beta(nu_\beta)=\sum_a h_a^{(1)}. \tag{A.17}$$

In view of matching the target dynamics Eqs. (2.10) and (2.12), the selection of $h_a^{(1)}$ becomes obvious:

$$h_a^{(1)}=-\frac{w_a n u_r}{r}\delta_t. \tag{A.18}$$

### A.2 Lattice momentum equation and $h_a^{(2)}$

Next we will determine $h_a^{(2)}$ with $h_a^{(1)}$ specified. After multiplication with $\zeta_{ai}$ and summation with respect to $a$, the different order momentum conservation equations are recovered below:

$$\sum_a\zeta_{ai}h_a^{(2)}=\delta_t\Big(1-\frac{1}{2\tau}\Big)\partial_{x_j}\sum_a\zeta_{ai}\zeta_{aj}f_a^{(1)}+\delta_t\partial_{t_2}nu_i+\frac{\delta_t}{2}\partial_{x_j}\Big(-\frac{nu_r\delta_t}{r}\Big)\delta_{ij}. \tag{A.19}$$

We first examine the term $\sum_a\zeta_{ai}\zeta_{aj}f_a^{(1)}$ and with Eq. (A.19), we have

$$\begin{aligned}&\sum_a\zeta_{ai}\zeta_{aj}f_a^{(1)}\\ =&-\tau\delta_t\partial_{t_1}\big(\sum_a\zeta_{ai}\zeta_{aj}f_a^{(0)}\big)-\tau\delta_t\partial_{x_k}\Big[n\Theta(u_i\delta_{jk}+u_j\delta_{ki}+u_k\delta_{ij})-\tau\delta_t\frac{nu_r}{r}\Big]\delta_{ij}.\end{aligned} \tag{A.20}$$

Assume the characteristic velocity, length and time of the flow problem are $U_c$, $L_c$, and $t_c$, respectively. Then $\partial_{t_1}(\sum_a \zeta_{ai}\zeta_{aj} f_a^{(0)})$ is of order $U_c^2/t_c$ and $\partial_{x_k}(n\Theta(u_i\delta_{jk}+u_j\delta_{ki}+u_k\delta_{ij}))$ is of order $U_c/L_c$, and we have

$$\frac{\partial_{t_1}\sum_a \zeta_{ai}\zeta_{aj} f_a^{(0)}}{\partial_{x_k} n\Theta(u_i\delta_{jk}+u_j\delta_{ki}+u_k\delta_{ij})}=\mathcal{O}(M^2). \tag{A.21}$$

Under the assumption $M \ll 1$, one can neglect the term $\partial_{t_1}\sum_a \zeta_{ai}\zeta_{aj} f_a^{(0)}$, and one has

$$\sum_a \zeta_{ai}\zeta_{aj} f_a^{(1)} = -\tau\delta_t n\Theta(\partial_{x_j}u_i+\partial_{x_i}u_j)+\tau\delta_t\frac{nu_r}{r}(\Theta-1)\delta_{ij}. \tag{A.22}$$

Substituting the above equation into Eq. (A.19), we obtain

$$\begin{aligned}\sum_a \zeta_{ai} h_a^{(2)} =& -\delta_t^2\tau n\Theta\Big(1-\frac{1}{2\tau}\Big)\Big(\frac{\partial^2 u_i}{\partial x_j^2}+\frac{\partial^2 u_j}{\partial x_i\partial x_j}\Big)\\ &+\delta_t^2\Big(1-\frac{1}{2\tau}\Big)\frac{\partial}{\partial x_j}\frac{\tau n u_r}{r}(\Theta-1)\delta_{ij}+\delta_t\frac{\partial}{\partial_{t_2}}nu_i-\frac{\delta_t^2}{2}\frac{\partial}{\partial x_i}\frac{nu_r}{r}.\end{aligned} \tag{A.23}$$

Using the relationship

$$\frac{\partial}{\partial t_1}nu_i=-\frac{\partial}{\partial x_j}n(\Theta\delta_{ij}+u_iu_j) \tag{A.24}$$

and after some algebra, we have

$$\begin{aligned}&n\delta_t\Big(\frac{\partial u_i}{\partial t}+\frac{\partial(u_iu_j)}{\partial x_j}+\frac{1}{n}\frac{\partial P}{\partial x_i}-\mu\frac{\partial^2 u_i}{\partial x_j^2}\Big)\\ =&-n\delta_t\mu\frac{\partial}{\partial x_i}\frac{u_r}{r}-\delta_t^2\Big(\frac{n\mu}{\delta_t}-n\tau\Big)\frac{\partial}{\partial x_i}\frac{u_r}{r}+\sum_a \zeta_{ai}h_a^{(2)},\end{aligned} \tag{A.25}$$

where $\mu=\delta_t(\tau-1/2)\Theta$. We have $h_a^{(2)}$:

$$h_a^{(2)}=n\Big[\delta_t\Big(-\frac{u_ru_j}{r}+\frac{\nu}{r}\frac{\partial u_j}{\partial r}-\frac{\nu u_r}{r^2}\delta_{ir}\Big)\zeta_{aj}w_a+(2\delta_t\mu-\delta_t^2\tau)w_a\zeta_{aj}\frac{\partial}{\partial x_j}\frac{u_r}{r}\Big]. \tag{A.26}$$

We also have

$$h_a^{(2)}=\frac{\delta_t^2}{2}nw_a\Big(\frac{\partial\Theta}{\partial r}+\frac{\partial}{\partial x_j}u_ru_j\Big). \tag{A.27}$$

Finally, we obtain

$$\begin{aligned}h_a^{(2)}=&\frac{\delta_t^2}{2}nw_a\Big(\frac{\partial}{\partial r}\Theta+\frac{\partial}{\partial x_j}u_ru_j\Big)+n\delta_t\Big(-\frac{u_ru_j}{r}+\frac{\mu}{r}\frac{\partial u_j}{\partial r}-\frac{\mu u_r}{r^2}\delta_{ir}\Big)\zeta_{aj}w_a\\ &+n(2\delta_t\mu-\delta_t^2\tau)w_a\zeta_{aj}\frac{\partial}{\partial x_j}\frac{u_r}{r}.\end{aligned} \tag{A.28}$$

Regroup the term $h_a^{(2)}$, we finally have Eq. (4.5).

## References


[1] G. McNamara and G. Zanetti, Use of the Boltzmann equation to simulate lattice-gas automata, Phys. Rev. Lett., 61 (1988), 2332–2335.

[2] Y. H Qian, D. D'Humieres, and P. Lallemand, Lattice BGK models for Navier-Stokes equation, Europhys. Lett., 17 (1992), 479–484.

[3] H. Chen, S. Chen, and W. H. Matthaeus, Recovery of the Navier-Stokes equations using a lattice-gas Boltzmann method, Phys. Rev. A., 45 (1992), R5339–R5342.

[4] Y. H. Qian, and S. A. Orszag, Lattice BGK models for the Navier-Stokes equation: nonlinear deviation in compressible regimes, Europhys. Lett., 21 (1993), 255–259.

[5] P. L. Bhatnagar, E. P. Gross, and M. Krook, A model for collision processes in gases I: small amplitude processes in charged and neutral one-component systems, Phys. Rev., 94 (1954), 511–525.

[6] D. H. Rothman, and S. Zaleski, Lattice-gas models of phase separation: interfaces, phase transitions, and multiphase flow, Rev. Mod. Phys., 66 (1994), 1417–1479.

[7] X. He, and L.-S. Luo, A priori derivation of the lattice Boltzmann equation, Phys. Rev. E., 55 (1997), R6333.

[8] L.-S. Luo, Comment on discrete Boltzmann equation for microfluidics, Phys. Rev. Lett., 92 (2004), 139401.

[9] X. Shan, and X. He, Discretization of the velocity space in the solution of the Boltzmann equation, Phys. Rev. Lett., 80 (1998), 65.

[10] X. Shan, X.-F. Yuan, and H. Chen, Kinetic theory representation of hydrodynamics: a way beyond the Navier-Stokes equation, J. Fluid. Mech., 550 (2006), 413.

[11] H. Grad, On the kinetic theory of rarefied gases, Commun. Pure. Appl. Math., 2 (1949), 331–407.

[12] G. Chen, Nanosclae Energy Transport and Conversion, Oxford University Press, 2005.

[13] E. A. Uehling, and G. E. Uhlenbeck, Transport phenomena in Einstein-Bose and Fermi-Dirac gases I, Phys. Rev., 43 (1933), 552–561.

[14] M. Lundstrom, Fundamentals of Carrier Transport, Cambridge University Press, 2nd ed., 2000.

[15] J. Y. Yang, and L. H. Hung, Lattice Uehling-Uhlenbeck Boltzmann-BGK hydrodynamics of quantum gases, Phys. Rev. E., 79 (2009), 056708.

[16] I. Halliday, L. A. Hammond, C. M. Care, K. Good, and A. Stevens, Lattice Boltzmann equation hydrodynamics, Phys. Rev. E., 64 (2001), 011208.

[17] Y. C. Peng, C. Shu, Y. T. Chew, and J. Qiu, Numerical investigation of flows in Czochralski crystal growth by an axisymmetric lattice Boltzmann method, J. Comput. Phys., 186 (2003), 295–307.

[18] X. D. Niu, C. Shu, and Y. T. Chew, An axisymmetric lattice Boltzmann model for simulation of Taylor-Couette flows between two concentric cylinders, Int. J. Mod. Phys. C., 6 (2003), 785–796.

[19] K. N. Premnath, and J. Abraham, Lattice Boltzmann model for axisymmetric multiphase flows, Phys. Rev. E., 71 (2005), 056706.

[20] T. S. Lee, H. Huang, and C. Shu, An axisymmetric incompressible lattice Boltzmann model for pipe flow, Int. J. Mod. Phys. C., 17 (2006), 645–661.

[21] T. Reis, and T. N. Philips, Modified lattice Boltzmann model for axisymmetric flows, Phys. Rev. E., 75 (2007), 056703.

[22] S. Mukherjee, and J. Abraham, Lattice-Boltzmann simulations of two-phase flow with high

density ratio in axially symmetric geometry, Phys. Rev. E., 75 (2007), 026701.

[23] T. Reis, and T. N. Philips, Erratum: modified lattice Boltzmann model for axisymmetric flows [Phys. Rev. E., 75 (2007), 056703], Phys. Rev. E., 76 (2007), 059902.

[24] T. Reis, and T. N. Philips, Numerical validation of a consistent axisymmetric lattice Boltzmann model, Phys. Rev. E., 77 (2008), 026703.

[25] J. G. Zhou, Axisymmetric lattice Boltzmann method, Phys. Rev. E., 78 (2008), 036701.

[26] Z. L. Guo, H. Han, B. Shi, and C. Zheng, Theory of the lattice Boltzmann equation: lattice Boltzmann model for axisymmetric flows, Phys. Rev. E., 79 (2009), 046708.

[27] M. Knudsen, The law of the molecular flow and viscosity of gases moving through tubes, Ann. Phys., 28 (1909), 75–130.

[28] M. Knudsen, The Kinetic Theory of Gases, Methuen & Co. London, 1934.

[29] Y. H. Shi, and J. Y. Yang, J. Comput. Phys., 343 (2008), 552.

[30] S. Chapman, and T. G. Cowling, The Mathematical Theory of Non-Uniform Gases, 3rd ed., Cambridge University Press, 1970.

[31] M. J. Rice, Size-dependent transport-coefficient effects in fermi liquids, Phys. Rev., 165 (1968), 288–292.

[32] B. C. Eu, Normal-stress effects in tube flow of a non-Newtonian fluid, Phys. Rev. A., 40 (1989), 1497–1506.

[33] J. M. Parpia, and T. L. Rhodes, First observation of the Knudsen minimum in normal liquid $^3He$, Phys. Rev. Lett., 5 (1983), 805–808.

[34] D. Sawkey, and J. P. Harrison, Volume flow in liquid $^3He$ in the Knudsen and Poiseuille regions, Phys. B., 112 (2003), 329–333.

[35] M. Kardar, Statistical Physics of Particles, Cambridge University Press, 2007.